Supporting Information to:

In situ formation of SERS hot spots by bis-quaternized perylene dye: a simple strategy for highly sensitive detection of heparin over a wide concentration range

Wei Ji, *[a] Xue Zhang,[a,b] Jianzhang Zhao,[b] Ye Gao,[a] Wei Song[c] and Yukihiro Ozaki[d]

a. School of Chemistry, Dalian University of Technology, Dalian 116024, P.R. China; Email: jiwei@dlut.edu.cn

b. State Key Laboratory of Fine Chemicals, School of Chemical Engineering, Dalian University of Technology, Dalian 116024, P.R. China.

c. State Key Laboratory of Supramolecular Structure and Materials, Jilin University, Changchun 130012, P.R. China

d. School of Science and Technology, Kwansei Gakuin University, 2-1 Gakuen, Sanda, Hyogo 669-1337, Japan.

1. EXPERIMENTAL SECTION

1.1 Synthesis of Raman probe. The Raman probe was synthesized following the literature procedures (Scheme S1)[1-3].

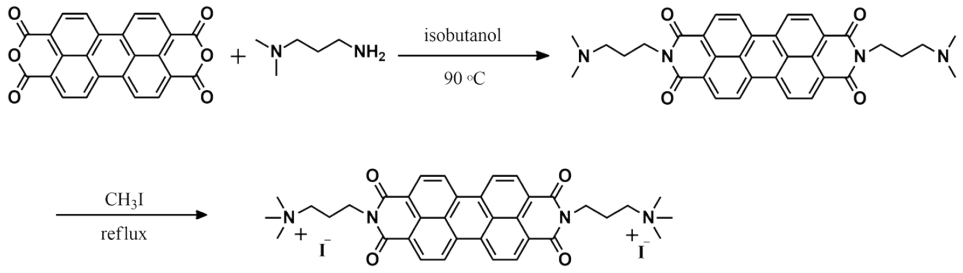

Scheme S1. Synthetic route for BQPER.

Synthesis of N,N′-bis[3,3′-(dimethylamino)propylamine]-3,4,9,10-perylenediimide (Compound 1)

3-dimethylaminopropylamine (15 mL, 118 mmol) and perylene tetracarboxylic dianhydride (PTCDA, 5.00 g, 12.1 mmol) were dissolved in isobutanol (200 mL) and the mixture was heated at 90 °C for 24 hours with stirring under N_2 atmosphere. After filtration, the residue was washed with deionized water and ethanol, and then the crude product was further treated with 5% aqueous NaOH solution at 90 °C for 30 min to remove the unreacted PTCDA. The suspended mixture was filtered, washed with deionized water and ethanol. After drying under vacuum, the compound 1 (6.05 g, yield: 89%) was obtained as a a red solid.

Synthesis of N,N′-bis[3,3′- (trimethylammonium)propylamine]- 3,4,9,10-perylenediimide (Bis-Quaternized Perylene dyes, abbreviation was defined as BQPER)

Compound 1 (3.0 g, mmol) and methyl iodide (4.5 mL, 72.2 mmol) were dissolved in toluene (150 mL) in a 250 mL round bottom flask. The mixture was refluxed for 3 hours under N_2 atmosphere, and then it was cooled to room temperature with stirring. After filtration, the residue was washed with ether and dried under vacuum to produce a brown-red solid (4.17 g, 90%). ^{1}H NMR (400 MHz, 80 °C, DMSO-d_6): δ (ppm) = 2.17–2.24 (m, 4H), 3.08 (s, 18H), 3.47–3.51 (m, 4H), 4.18–4.21 (t, 4H, J = 6.6 Hz), 8.53–8.55 (d, 4H, J = 7.8 Hz), 8.81–8.84 (d, 4H, J = 7.9 Hz). ESI-MS: *m/z* calcd for $[C_{36}H_{38}N_4O_4]^{2+}$: 259.1; found: 295.2.

1.2 Finite-difference time domain (FDTD) simulation.

The electric-field distribution was simulated by commercial software, FDTD Solutions (Lumerical Solutions, Inc.), which is based on 3D-finite-difference time-domain (3D-FDTD) method. Optical constants for bulk Ag were adapted from Palik's database. The model used for simulation was sphere Ag

NP with diameter of 60 nm. The gap between the Ag dimer was set as 2 nm to fit with the size of BQPER. The FDTD simulation volume was 1 μm (x) by 1 μm (y) by 1 μm (z) and the minimum mesh step was set as 0.1 nm. Perfectly matched layer and periodic boundary conditions were used for the simulation. A plane wave of 785 nm propagating along the negative z-axis direction was used as the excitation source, and the polarization of the excitation source was along the x-axis.

1.3 Calculation of limit of detection (LOD).

The standard curve of heparin was plotted as

$$Y = A + B \times \log_{10} X \qquad (1)$$

where *A* and *B* are the variable obtained via least-square root linear regression for the signal-concentration curve, and *Y* is the SERS signal with heparin concentration of *X*. The limit of detection (LOD) is estimated at least three times higher than background noise. Thus, the maximum value of Y_{max} can be defined as:

$$Y_{max} = Y_{blank} - 3SD \qquad (2)$$

where Y_{blank} and SD are the SERS signal and standard deviation of blank sample (BQPER-Ag NPs), respectively. Then, the LOD can be calculated as:

$$LOD = 10^{\left[\left(Y_{blank} - 3SD\right) - A\right]/B} \qquad (3)$$

Inserting corresponding value into equation 3, LOD is calculated to be 0.08 ng/mL.

2. ADDITIONAL FIGURES AND TABLES

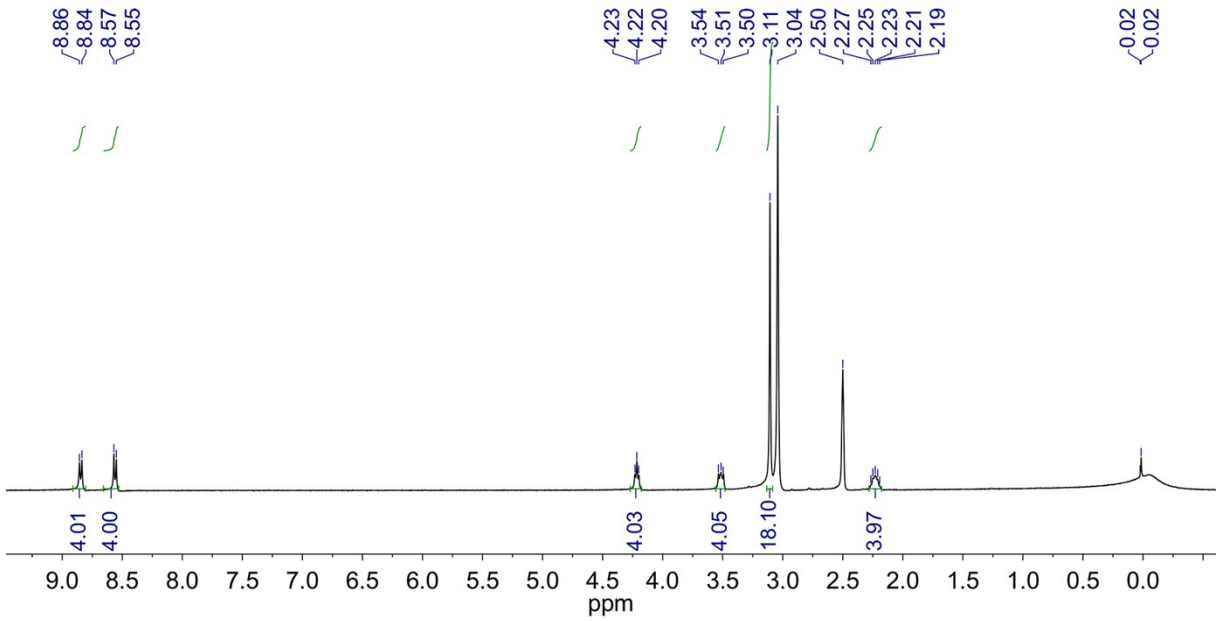

Fig. S1 ^{1}H NMR specturm of the BQPER.

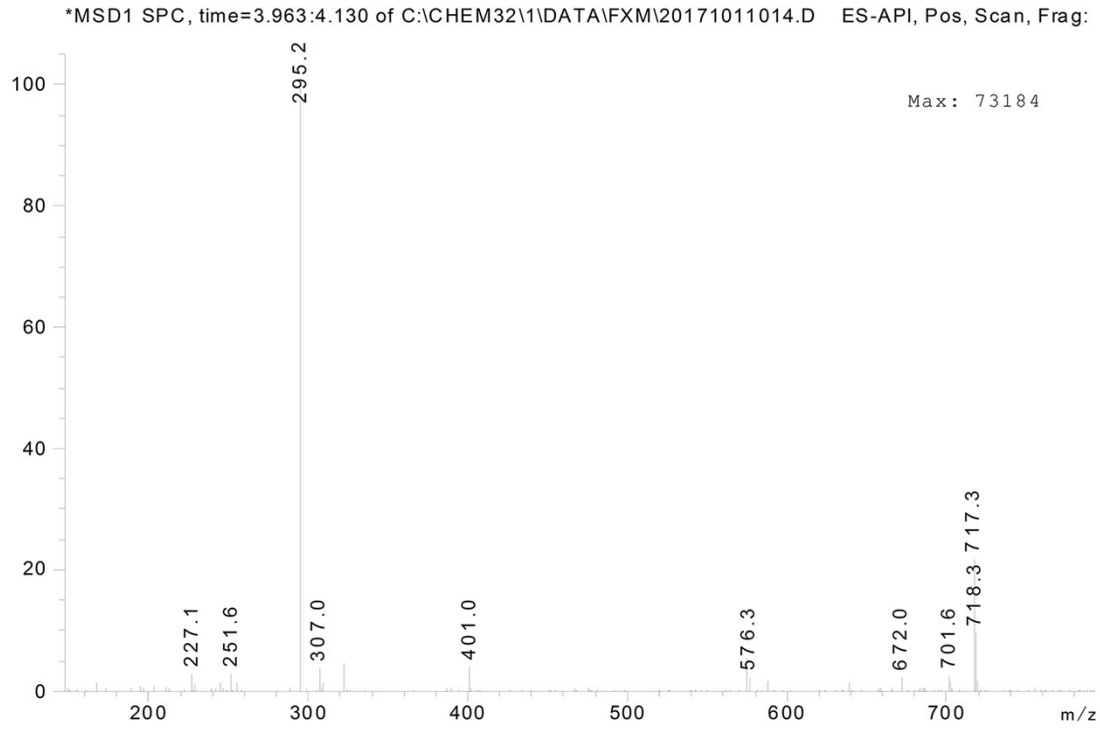

Fig. S2 ESI-MS of BQPER.

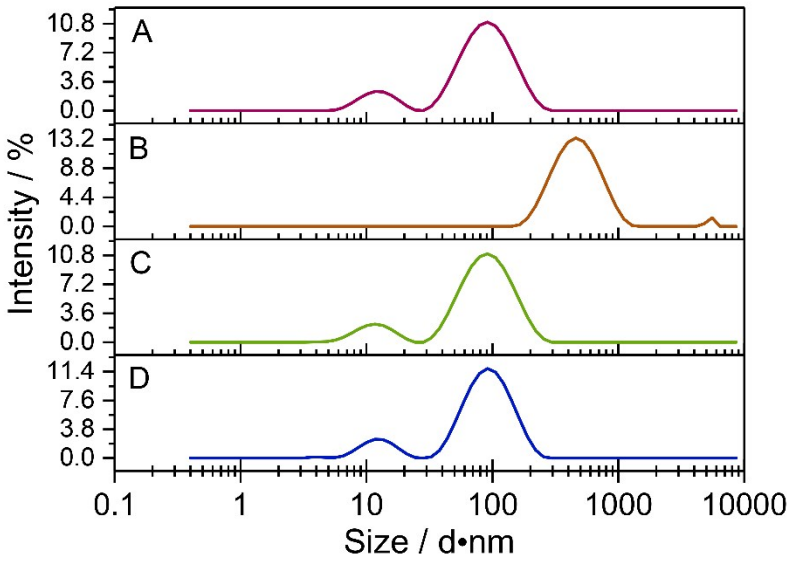

Fig. S3 Dynamic light scattering (DLS) analysis of Ag NPs without (A) and with (B) BQPER. (C) DLS analysis of Ag NPs with BQPER in the presence of heparin. (D) DLS analysis of Ag NPs with heparin. It was found that the size distribution of Ag NPs ranges from 10 to 200 nm. The average hydrodynamic diameter of Ag NPs is 52.5 nm, which is identical to that observed previously for Ag NPs synthesized by trisodium citrate. In contrast, the average hydrodynamic diameter of Ag NPs is 407.7 nm after addition of BQPER, indicating the formation of Ag aggregates. In the presence of heparin, the addition of BQPER does not induce any obvious variation in the hydrodynamic diameter of Ag NPs. These data further confirmed the formation of Ag aggregates after addition of BQPER, corresponding to the results of the UV-vis spectra and TEM images.

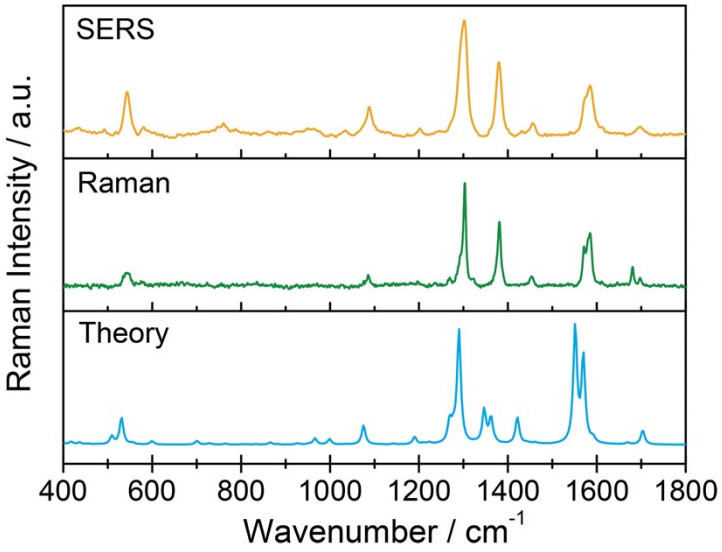

Fig. S4 Calculated Raman, experimental Raman, and SERS spectra of BQPER probe excited by a 785 nm laser. A line width of 10 cm^{-1} were used in the simulated Raman spectrum.

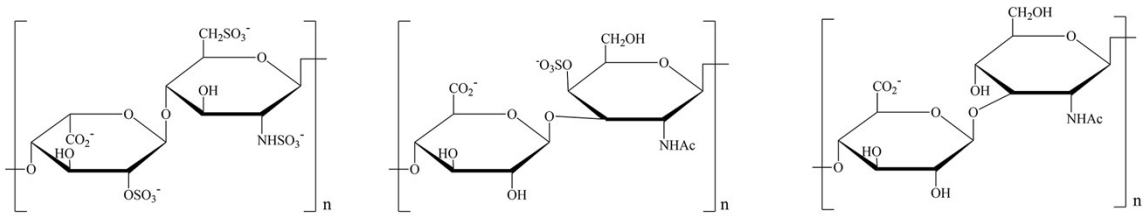

Fig. S5 Chemical structure of heparin, chondroitin sulfate (Chs), and hyaluronic acid (HA). Heparin, CHs, and HA have simlar conformation of the sugar dimer, but heparin has the higher anionic charge to mass ration in compared with Chs and HA.

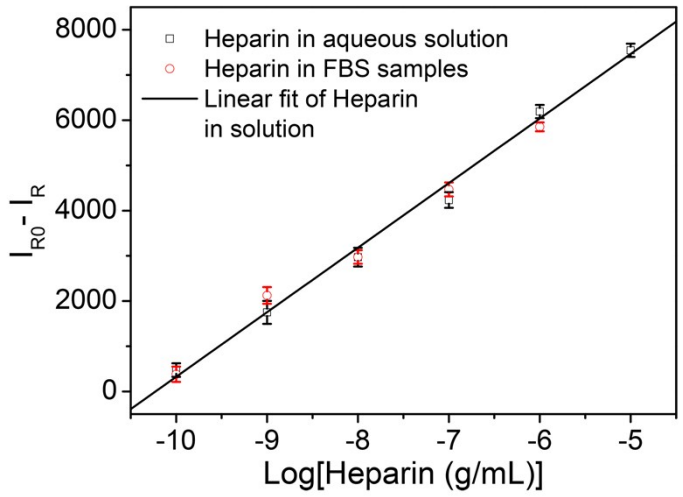

Fig.S6 Variation of the SERS intensities of BQPER with different concentration of heparin in aqueous solution (□) and FBS sample (○). The SERS intensity of BQPER without and with heparin were defined as I_0 and I, respectively. The substration of I_0 and I was used as the vertical coordinates for backgroud correction. In this way, it was clearly found that the background originated from FBS can be largely reduced.

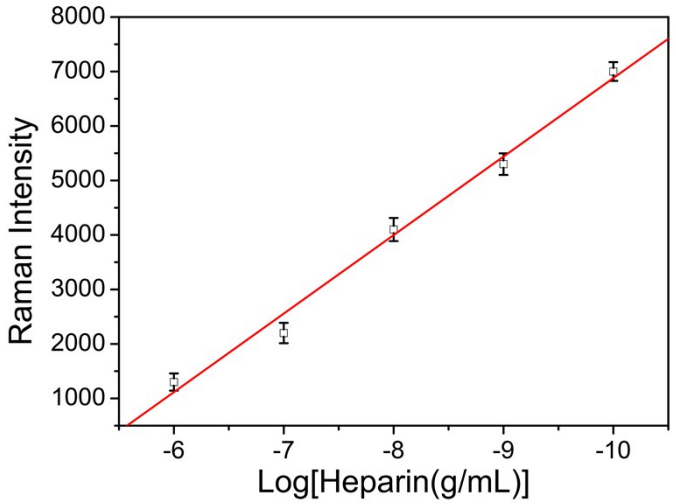

Fig. S7 Linear calibration curve for the heparin concentration in the range of 10^{-6} to 10^{-10} g/mL for 10^4-fold diluted human serum samples.

Table S1. Theoretical and Experimental Frequencies of Fundamental Vibrational Bands of BQPER within the Wavenumber Range of 400-1800 cm^{-1}

theory [a,b]	experiment [b]		assignment [e]
	Raman [c]	SERS [d]	
1702	1697	1698	ν_{CO}
1569	1585	1585	ν_{CC}
1551	1571	1573	ν_{CC}
1422	1453	1457	$\nu_{CC} + \beta_{CH} + \nu_{CN}$
1362	1381	1379	$\nu_{CC} + \nu_{CN} + \beta_{CH}$
1346			$\nu_{CC} + \beta_{CH}$
1290	1308	1303	$\nu_{CC} + \beta_{CH}$
1190	1197	1201	$\beta_{CH} + \nu_{CN}$
1075	1086	1088	$\beta_{CH} + \nu_{CN}$
532	541	543	α_{CCC}

[a] Calculated normal Raman bands of BQPER by using DFT B3LYP method. [b] An excitation wavelength of 785 nm were used both in the simulated and experiment spectra. [c] The Raman bands were measured in solid. [d] The SERS bands were measured by using Ag NPs as the substrate material. [e] Approximate description of the vibrational modes (ν, stretching; β, bending; α, ring deformation).

Table S2 Summary of Typical Heparin Sensors.

	mechanism	linear range [a]	limit of detection	ref.
1	Turn-off SERS	0.1–10000ng/mL (0.0185 U/mL–18.5 U/mL)	0.08 ng/mL (0.0009 U/mL)	This work
2	Turn-off SERS	0.5–150 ng/mL	0.5 ng/mL	4
3	Turn-off SERS	0.05–20 ng/mL	0.03 ng/mL	5
4	Turn-off SERS	0.2–2.4 U/mL	0.042 U/mL	6
5	Resonance Rayleigh scattering	8.25–2500 ng/mL	2.48 ng/mL	7
6	Resonance Rayleigh scattering	0.001–0.15 U/mL	0.0005 U/mL	8
7	Turn-off fluorescence	20–2000 ng/mL	18 ng/mL	9
8	Turn-off luminescence	0.4–100 μM	0.22 μM	10
9	Turn-off fluorescence	0.18–18 μg/mL	75 ng/mL	11
10	Turn-on fluorescence	4–1600 ng/mL	1.3 ng/mL	12
11	Turn-on fluorescence	0.2–5 μg/mL	33 ng/mL	13
12	Turn-on fluorescence	0.1–60 nM	0.036 nM	14
13	Turn-on fluorescence	0.04–1.6 μg/mL	0.02 μg/mL	15
14	Turn-on fluorescence	0.18–1.8 μg/mL	60 ng/mL	16
15	Ratiometric fluorescence	0-50 pM	3 pM	17
16	Ratiometric fluorescence	0–7 nM	763 pM	18
17	Ratiometric fluorescence	1–10 μM	Not available	19
18	Ratiometric fluorescence	0–70 nM	2.46 nM	20
19	Ratiometric fluorescence	Not available	0.02 U/mL	21
20	Aggregation induced emission	1–12 μM	23 nM	22
21	Aggregation induced emission	0–15 μM	26 nM	23
22	Aggregation induced emission	0–14 μM	22 nM	24
23	Time-resolved luminescence	0.01–1 μg/mL	4.6 ng/mL	25
24	Luminescence	0–3.6 μg/mL	12.5 ng/mL	26
25	UV-visible absorption	0–6.4 U/mL	0.0142 U/mL	27

[a] The molecular weight (MWs) of heparin cannot be described by a single number due to its natural polydispersity and the specification of heparin is usually described by its activity unit. Thus, the mass concentration of heparin cannot be directly converted into molarity. However, it was clealy found that the liner range of this work is wider than other currently used assays for heparin concetration determination.

References

1. T. Deligeorgiev, D. Zaneva, I. Petkov, I. Timcheva and R. Sabnis, *Dyes. Pigm.*, 1994, **24**, 75-81.
2. Z.-R. Liu and R. L. Rill, *Anal. Biochem.*, 1996, **236**, 139-145.
3. B. Wang and C. Yu, *Angew. Chem. Int. Edit.*, 2010, **49**, 1485-1488.
4. X. Wang, L. Chen, X. Fu, L. Chen and Y. Ding, *ACS Appl. Mater. Inter.*, 2013, **5**, 11059-11065.
5. C. Zhang, X. Liang, T. You, N. Yang, Y. Gao and P. Yin, *Anal. Methods*, 2017, **9**, 2517-2522.
6. G. Qu, G. Zhang, Z. Wu, A. Shen, J. Wang and J. Hu, *Biosens. Bioelectron.*, 2014, **60**, 124-129.
7. S. Yan, Y. Tang and M. Yu, *RSC Adv.*, 2015, **5**, 59603-59608.
8. Y. Ling, Z. F. Gao, Q. Zhou, N. B. Li and H. Q. Luo, *Anal. Chem.*, 2015, **87**, 1575-1581.
9. S. D. Ma, Y. L. Chen, J. Feng, J. J. Liu, X. W. Zuo and X. G. Chen, *Anal. Chem.*, 2016, **88**, 10474-10481.
10. J. Li, M. Cheng and M.-J. Li, *Analyst*, 2017, **142**, 3733-3739.
11. S.-Y. Hung and W.-L. Tseng, *Biosens. Bioelectron.*, 2014, **57**, 186-191.
12. J. Zhao, Y. Yi, N. Mi, B. Yin, M. Wei, Q. Chen, H. Li, Y. Zhang and S. Yao, *Talanta*, 2013, **116**, 951-957.
13. H. Z. Zhang, R. S. Li, N. Wang, L. Qi, C. Z. Huang and J. Wang, *Anal. Methods*, 2016, **8**, 453-459.
14. Y. Wang, Z. Wu and Z. Liu, *Anal. Chem.*, 2013, **85**, 258-264.
15. Y. Li, H. Sun, F. Shi, N. Cai, L. Lu and X. Su, *Biosens. Bioelectron.*, 2015, **74**, 284-290.
16. C.-Y. Kuo and W.-L. Tseng, *Chem. Commun.*, 2013, **49**, 4607-4609.
17. D.-H. Kim, Y. J. Park, K. H. Jung and K.-H. Lee, *Anal. Chem.*, 2014, **86**, 6580-6586.
18. P. Thirupathi, J.-Y. Park, L. N. Neupane, M. Y. L. N. Kishore and K.-H. Lee, *ACS Appl. Mater. Inter.*, 2015, **7**, 14243-14253.
19. C. W. Chan and D. K. Smith, *Chem. Commun.*, 2016, **52**, 3785-3788.
20. P. K. Mehta, H. Lee and K.-H. Lee, *Biosens. Bioelectron.*, 2017, **91**, 545-552.
21. L. Zhao, T. Wang, Q. Wu, Y. Liu, Z. Chen and X. Li, *ACS Appl. Mater. Inter.*, 2017, **9**, 3400-3410.
22. M. Wang, D. Zhang, G. Zhang and D. Zhu, *Chem. Commun.*, 2008, DOI: 10.1039/B808877B, 4469-4471.
23. N. H. Mudliar and P. K. Singh, *ACS Appl. Mater. Inter.*, 2016, **8**, 31505-31509.
24. S. Li, M. Gao, S. Wang, R. Hu, Z. Zhao, A. Qin and B. Z. Tang, *Chem. Commun.*, 2017, **53**, 4795-4798.

25. Y. Hu, W. Guo, Y. Ding, H. Cheng and H. Wei, *Biosens. Bioelectron.*, 2016, **86**, 858-863.

26. N. Dey, S. K. Samanta and S. Bhattacharya, *Chem. Commun.*, 2017, **53**, 1486-1489.

27. J. Wang, F. Chen, S. J. Arconada-Alvarez, J. Hartanto, L.-P. Yap, R. Park, F. Wang, I. Vorobyova, G. Dagliyan, P. S. Conti and J. V. Jokerst, *Nano Lett.*, 2016, **16**, 6265-6271.